

## 结晶性和粒子尺寸对 C<sub>60</sub> 薄膜晶体管迁移率的影响

李 谊 韩 笑 孙志鹏 马延文\*  
(南京邮电大学材料科学与工程学院, 南京 210023)

**摘要:** 采用真空沉积方法在不同基片温度(30~190 °C)和沉积压力( $1 \times 10^{-4}$  和  $1 \times 10^{-1}$  Pa)下制得了 C<sub>60</sub> 薄膜。研究了薄膜的结晶性和晶粒尺寸对迁移率的影响。采用 X 射线衍射和原子力显微镜表征了薄膜的结构和形貌,发现提高基片温度,薄膜的结晶性和晶粒尺寸均提高;提高沉积压力,薄膜的晶粒尺寸增大而结晶性不变。场效应测试结果表明,C<sub>60</sub> 薄膜的迁移率与其结晶性密切相关,高的结晶性有利于获得高迁移率;不同于平面有机半导体材料,对于球状 C<sub>60</sub> 半导体材料,大的晶粒尺寸可能导致低迁移率。

**关键词:** 富勒烯; 薄膜晶体管; 迁移率; 结晶性; 晶粒尺寸

中图分类号: O613.71 文献标识码: A 文章编号: 1001-4861(2018)03-0415-06

DOI: 10.11862/CJIC.2018.076

## Effect of Crystallinity and Grain Size of Film on Mobility of C<sub>60</sub> Thin Film Transistors

LI Yi HAN Xiao SUN Zhi-Peng MA Yan-Wen\*  
(Institute of Advanced Materials, Nanjing University of Posts and Telecommunications, Nanjing 210023, China)

**Abstract:** Fullerene (C<sub>60</sub>) thin films have been prepared on SiO<sub>2</sub> substrates by vacuum deposition under different substrate temperature ranging from 30 to 190 °C and deposition pressure of  $1 \times 10^{-4}$  and  $1 \times 10^{-1}$  Pa. The effect of crystallinity and grain size on the mobility of the deposited C<sub>60</sub> thin films are investigated. X-ray diffraction and atomic force microscopy observation indicates that both the crystallinity and the grain size of the C<sub>60</sub> films increase with increasing substrate temperature. And the grain size of the films increase and the crystallinity keep almost unchanged with increasing deposition pressure. Field-effect measurements indicate that the mobilities of the C<sub>60</sub> thin films are closely correlated with their crystallinities, and the increased crystallinity of the films gives the improved mobility. Different from the films of planar organic semiconductor molecules, for the spherical C<sub>60</sub> molecules films, the larger grain size could lead to the lower mobility.

**Keywords:** fullerene; thin film transistors; mobility; crystallinity; grain size

## 0 Introduction

In recent decades, organic thin film transistors (OTFTs) have received considerable attention owing to their low cost, low temperature process, compatibility with plastic substrate, and wide potential applications in large-area, lightweight, flexible electronics devices such as electronic displays, organic memories, and

sensors<sup>[1-5]</sup>. Much research work has been focused on obtaining high performance OTFTs comparable to those of amorphous silicon thin film transistors (TFTs)<sup>[6-10]</sup>. In addition to the optimization of device structure and performance, the correlation of the charge transport with the thin-film microstructure has also been extensively studied. It is well known that the charge transfer in OTFTs highly rely on the crystallinity,

收稿日期: 2017-08-31。收修改稿日期: 2017-11-27。

国家自然科学基金(No.61504062)、江苏省自然科学基金(No.BK20150863)和南京邮电大学引进人才基金(No.NY214183)资助项目。

\*通信联系人。E-mail: iamywma@njupt.edu.cn

molecular ordering and crystal grain sizes, which in turn depend on the molecular structures of the organic semiconductors<sup>[11-12]</sup>, deposition process<sup>[13-16]</sup>, and substrates<sup>[17-18]</sup>. For the most planar organic semiconductor molecules, such as CuPc, F<sub>16</sub>CuPc, pentacene, perylene bisimide and oligothiophene, increasing substrate temperature ( $T_s$ ), decreasing deposition rate, and increasing deposition pressure in vacuum deposition process normally leads to a highly ordered film with larger grain sizes and fewer grain boundaries, which is regarded as the most effective way to obtain high-mobility devices<sup>[14-25]</sup>. However, for the spherical C<sub>60</sub> semiconductor, which is an important n-type semiconductor material with high mobility, the mechanism of charge transport in C<sub>60</sub> films is still unclear, and the relationship between mobility and microstructure of the C<sub>60</sub> films is controversial<sup>[20,26-28]</sup>. Therefore, it is essential to investigate the effect of morphology and structure, which are quite sensitive to growth conditions, on the performance of the C<sub>60</sub> films in-depth. In this study, the crystallinity and grain size of the C<sub>60</sub> films have been regulated by changing the  $T_s$  and deposition pressure in the vacuum deposition process. X-ray diffraction (XRD) and atomic force microscopy (AFM) were used to investigate the morphology and crystalline structure of thin films. Furthermore, the mobilities of the films are obtained by field-effect measurements, and the correlations of mobility with crystallinity and grain size of the C<sub>60</sub> films are established.

## 1 Experimental

### 1.1 Fabrication of C<sub>60</sub> TFTs

Fig.1 shows the schematic diagram of the fabricated C<sub>60</sub> TFTs. C<sub>60</sub> (99.9%) is purchased from Aldrich and used without further purification. The substrate is 300 nm SiO<sub>2</sub> thermally grown on a heavily doped n-Si wafer, which were ultrasonically cleaned with acetone, isopropyl alcohol, and ultrapurified water, successively. A bottom-gate, top-contact device configuration of C<sub>60</sub> TFTs was adopted. First, the substrate was set in the chamber and maintained at  $4 \times 10^{-5}$  Pa. Subsequently, a 40 nm thick C<sub>60</sub> active

layer<sup>[16]</sup>, patterned through a shadow mask, was deposited by vacuum evaporation onto the substrate under a specific  $T_s$  (i.e., 30, 60, 90, 130, 160 and 190 °C) at the same rate of  $0.01 \text{ nm} \cdot \text{s}^{-1}$  recorded by a quartz crystal oscillator. Finally, the gold (Au, 99.99%) electrodes, with a thickness of 50 nm, were defined on the C<sub>60</sub> film by thermal evaporation through another mask. For the samples of different deposition pressure, the films were deposited by vacuum deposition under a specific  $P_{\text{dep}}$  (i.e.  $1 \times 10^{-4}$  and  $1 \times 10^{-1}$  Pa) with the rate of  $0.01 \text{ nm} \cdot \text{s}^{-1}$  and the  $T_s$  of 130 °C. The channel length ( $L$ ) and width ( $W$ ) are 70 and 500  $\mu\text{m}$ , respectively.

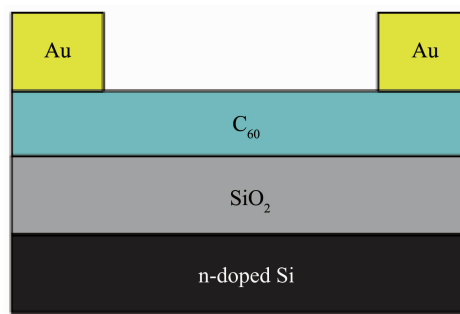


Fig.1 Schematic diagram of the fabricated C<sub>60</sub> TFTs

### 1.2 Characterization

The structures and surface morphologies of the films were characterized by X-ray diffraction (XRD, Philips X'pert Pro X-ray diffractometer in  $2\theta$  range of  $15^\circ \sim 28^\circ$ , Cu  $K\alpha_1$  radiation of 0.154 nm) and atomic force microscopy (AFM, Bruker Dimension Icon, tapping Mode). The performances of the devices were evaluated by semiconductor characterization system (Keithley model 4200-SCS) under vacuum condition at room temperature.

## 2 Results and discussion

### 2.1 Surface morphology and structure of C<sub>60</sub> films

The characteristic XRD patterns and morphologies of the C<sub>60</sub> films deposited under different  $T_s$  are shown in Fig.2. The XRD patterns of the C<sub>60</sub> films show broadened (113) peaks, corresponding to the  $D$  values of *ca.* 1.54 nm. With increasing  $T_s$  from 30 to 190 °C, the intensity of (113) peaks increase, indicating the increased crystallinity of the films (Fig.2A). The

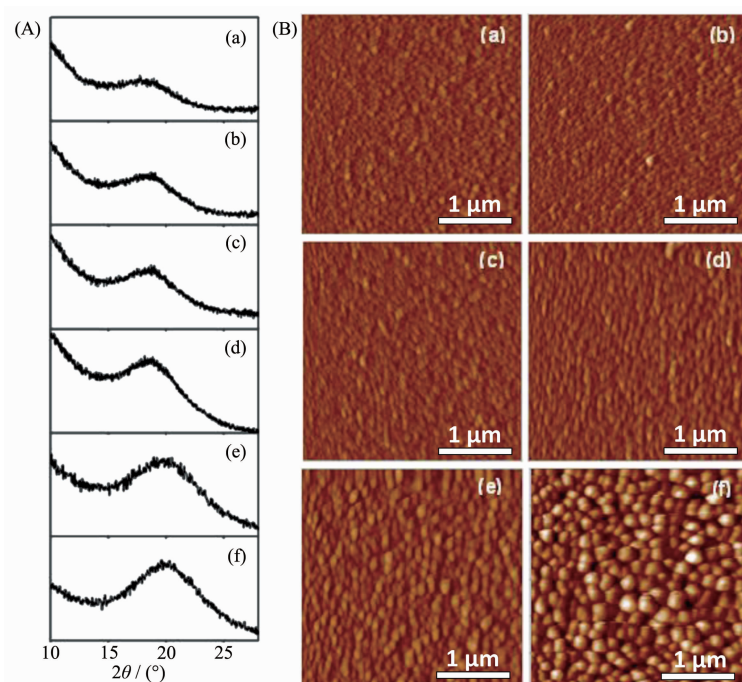


Fig.2 Characteristic XRD patterns (A) and AFM images (B) of the 40 nm  $C_{60}$  films deposited under different  $T_s$  of 30, 60, 90, 130, 160 and 190 °C (a~f), respectively

morphological evolutions of the  $C_{60}$  films with  $T_s$  are demonstrated in Fig.2B. It is clearly seen, the grain sizes keep almost unchanged for  $T_s$  below 90 °C (Fig. 2B(a~c)), and gradually increase for further increasing  $T_s$  from 90 to 190 °C (Fig.2B(d~f)). The root-mean-square roughness of all the samples obtained from the AFM measurements are about 1~3 nm, indicating the smooth surfaces of the films.

## 2.2 Electronic properties of $C_{60}$ films

Fig.3 shows the output characteristics of  $C_{60}$  TFTs prepared under different  $T_s$ . The  $C_{60}$  TFTs exhibit typical n-channel field-effect behavior, operated under a positive voltage source-drain voltage ( $V_d$ ) and gate voltage ( $V_g$ ), with distinct linear and saturation regions in the output curves. With increasing  $T_s$  from 30 to 130 °C, a significant increase of saturation drain current ( $I_d$ ) from 1.8 to 12.3  $\mu A$  is observed when they are

biased at  $V_d=60$  V and  $V_g=60$  V (Fig.3a~d). With further increasing  $T_s$  to 160 and 190 °C,  $I_d$  decreases to 4.2  $\mu A$  and 2.1  $\mu A$ , respectively.

Fig.4 shows the transfer characteristics of  $C_{60}$  TFTs prepared under different  $T_s$ . From the transfer curves, the carrier mobility are extracted for each device, and the relationship between the mobilities and  $T_s$  are shown in Fig.6. In order to make clear of the correlation of the mobilities with the corresponding crystallinity and morphologies of the  $C_{60}$  films, the changes of (113) peak intensity and grain sizes with  $T_s$  are re-plotted here. It is seen that, for  $C_{60}$  films with  $T_s$  below 130 °C, the mobilities increase from 0.026 to 0.211  $cm^2 \cdot V^{-1} \cdot s^{-1}$  with increasing  $T_s$ . With further increasing  $T_s$  to 160 and 190 °C, mobilities decrease to 0.082 and 0.030  $cm^2 \cdot V^{-1} \cdot s^{-1}$ , respectively. Because of the unchanged grain sizes of  $C_{60}$  films deposited

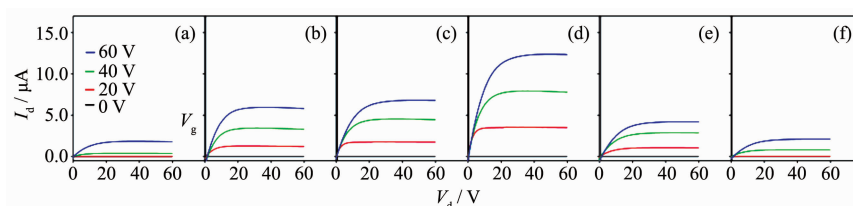


Fig.3 Output ( $I_d$ - $V_d$ ) characteristics of  $C_{60}$  TFTs prepared under different  $T_s$  of 30, 60, 90, 130, 160 and 190 °C (a~f)

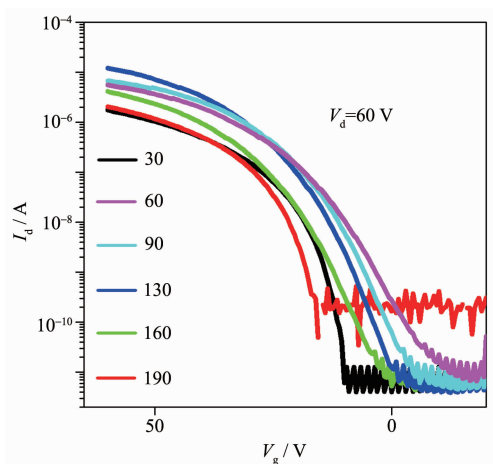


Fig.4 Transfer ( $I_d$ - $V_g$ ) characteristics of  $C_{60}$  TFTs prepared under different  $T_s$  of 30, 60, 90, 130, 160 and 190  $^{\circ}\text{C}$

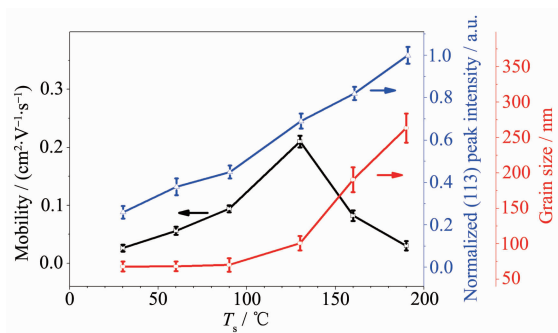


Fig.5 Carrier mobilities, grain sizes, and crystallinities ((113) peak intensity) of  $C_{60}$  thin films as functions of  $T_s$

under 30, 60 and 90  $^{\circ}\text{C}$ , the increase of mobilities could be attributed to the increased crystallinities of films. When  $T_s$  is up to 130  $^{\circ}\text{C}$ , the larger mobility was achieved mainly due to the higher crystallinities despite the slightly increased grain sizes. Interestingly, for the films with  $T_s$  of 160 and 190  $^{\circ}\text{C}$ , despite the increases in the crystallinities, remarkable decreased mobilities are obtained, which should be related the

obviously increased grain sizes. These results suggest the different grain-boundary effect for the spherical  $C_{60}$  molecules from that for the planar molecules, such as CuPc, pentacene, TIPS-pentacene, perylene bisimide and oligothiophene<sup>[14-25]</sup>. For the planar molecules, the grain boundary is a crucial barrier for the carrier transport, since the intermolecular charge hopping across the grain boundaries is less efficient than that within the grains. Thus, reducing the grain boundaries by increasing grain sizes is a promising approach to improve charge transport and mobility. However, for the  $C_{60}$  samples with  $T_s$  of 160 and 190  $^{\circ}\text{C}$ , the larger grain sizes of spherical  $C_{60}$  films lead to the lower mobilities, which is interesting and worth further investigating.

In order to reveal the influence of grain sizes on the mobilities of  $C_{60}$  films, the samples with similar crystallinities and different grain sizes are needed. In our previous study, we have demonstrated that higher deposition pressure in vacuum deposition could lead to the larger grain sizes of  $C_{60}$  films with unchanged crystallinities and molecular packing<sup>[16]</sup>. Thus, the  $C_{60}$  films with deposition pressure of  $1 \times 10^{-1}$  Pa and  $T_s$  of 130  $^{\circ}\text{C}$  are deposited and investigated. In contrast to the  $C_{60}$  films with deposition pressure of  $1 \times 10^{-4}$  Pa (Fig.2Ad and 2Bd), the samples of  $1 \times 10^{-1}$  Pa show the unchanged crystallinities and increased grain sizes, as shown in Fig.6. The  $C_{60}$  films with deposition pressure of  $1 \times 10^{-1}$  Pa have a mobility of  $0.030 \text{ cm}^2 \cdot \text{V}^{-1} \cdot \text{s}^{-1}$ , which is lower than the value of samples with deposition pressure of  $1 \times 10^{-4}$  Pa. Due to the unchanged crystallinities, the decrease of mobility should be corrected to the increased grain size.

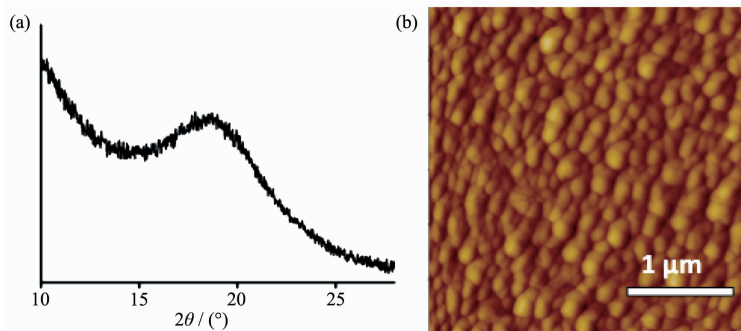


Fig.6 Characteristic XRD pattern (a) and AFM image (b) of the 40 nm  $C_{60}$  films deposited under  $1 \times 10^{-1}$  Pa and 130  $^{\circ}\text{C}$

As known, the performance of OTFTs is determined by the crystalline order and grain sizes of the first few molecular layers of the semiconductor near the semiconductor/dielectric interface. To ascertain the grain sizes of the  $C_{60}$  layers at  $C_{60}/SiO_2$  interface, two  $C_{60}$  films of 10 nm thickness were deposited on  $SiO_2$  at deposition pressure of  $1 \times 10^{-4}$  and  $1 \times 10^{-1}$  Pa, respectively. From the corresponding AFM images in Fig.7a and b, it is seen that, the 10 nm  $C_{60}$  films deposited under  $1 \times 10^{-4}$  Pa have a lot of small grains, while some larger grains are observed for the films of  $1 \times 10^{-1}$  Pa. This confirmed that larger grain sizes of  $C_{60}$  films result in the lower mobilities. The

possible mechanism for the effect of grain size on mobility of  $C_{60}$  films is proposed in Fig.7c and d. For the spherical  $C_{60}$  molecules, carrier could be effectively transported through nearest-neighbor hopping between molecules<sup>[26]</sup>. So the films with small and close grains are advantageous to effective charge transport (Fig.7c). For the films with large grain size, it is difficult to realize the nearest-neighbor hopping between grains (Fig.7d). Thus, the grain boundary is not a serious barrier for the charge transport, and the larger grain size could lead to the lower mobility in  $C_{60}$  TFTs.

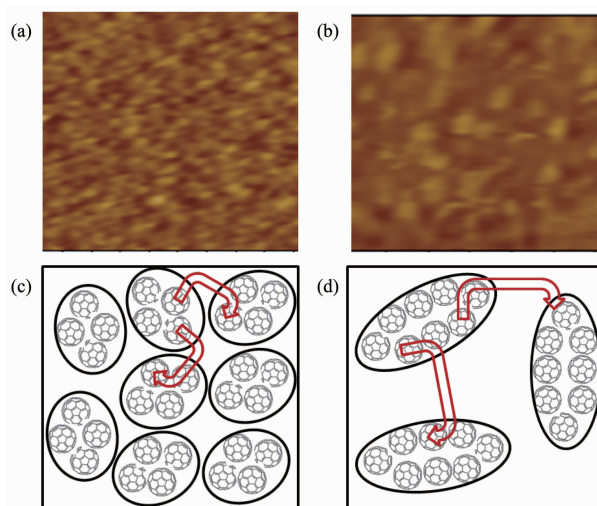


Fig.7 AFM images of 10 nm  $C_{60}$  films deposited under (a)  $1 \times 10^{-4}$  and (b)  $1 \times 10^{-1}$  Pa, and the possible charge transfer mechanism of  $C_{60}$  films with different grain size (c, d)

### 3 Conclusions

In summary,  $C_{60}$  films have been prepared on  $SiO_2$  substrates by vacuum deposition under different substrate temperature ranging from 30 to 190 °C and deposition pressure of  $1 \times 10^{-4}$  and  $1 \times 10^{-1}$  Pa. The experimental results indicate that the crystallinity and grain size of the  $C_{60}$  films thereof the mobility of the obtained TFTs could be effectively regulated by tuning substrate temperature and deposition pressure. A clear correlation of mobility with crystallinity and grain size of the  $C_{60}$  film is established. It is found that, both the crystallinity and the grain size of the  $C_{60}$  films increase with increasing substrate temperature. And the grain sizes of the films increase and the crystallinity keep almost unchanged

with increasing deposition pressure. The mobilities of the  $C_{60}$  films are closely correlated with the crystallinity and grain size. The increased crystallinity of the  $C_{60}$  films gives the improved mobility. Different from the films of planar organic semiconductor molecules, for the spherical  $C_{60}$  molecules films, the larger grain size could lead to the lower mobility. This study is helpful for the understanding of the charge transfer process and improving the performance of OTFTs.

### References:

- [1] Someya T, Bao Z, Malliaras G G. *Nature*, **2016**,**540**:379-385
- [2] Nomura K, Ohta H, Takagi A, et al. *Nature*, **2004**,**432**:488-492
- [3] Baeg K, Khim D, Kim J, et al. *Adv. Funct. Mater.*, **2012**,**22**:

- 2915-2926
- [4] Someya T, Sekitani T, Iba S, et al. *Proc. Natl. Acad. Sci. USA*, **2004**,**101**:9966-9970
- [5] Rotzoll R, Mohapatra S, Olariu V, et al. *Appl. Phys. Lett.*, **2006**,**88**:123502
- [6] Li Y, Liu Q, Wang X Z, et al. *Sci. China. Tech. Sci.*, **2012**, **55**:417-420
- [7] Sun X, Zhang L, Di C, et al. *Adv. Mater.*, **2011**,**23**:3128-3133
- [8] Virkar A, Mannsfeld S, Toney M F, et al. *Adv. Funct. Mater.*, **2009**,**19**:1962-1970
- [9] LI Yi(李谊), LIU Qi(刘琪), CAI Jing(蔡婧), et al. *Chinese J. Inorg. Chem.*(无机化学学报), **2014**,**11**:2621-2625
- [10] Kelley T W, Boardman L D, Dunbar T D, et al. *J. Phys. Chem. B*, **2003**,**107**:5877-5881
- [11] Facchetti A, Letizia J, Yoon M H, et al. *Chem. Mater.*, **2004**, **16**:4715-4727
- [12] Zhang X R, Richter L J, DeLongchamp D M, et al. *J. Am. Chem. Soc.*, **2011**,**133**:15073-15084
- [13] Li L, Hu W, Fuchs H, et al. *Adv. Energy Mater.*, **2011**,**1**: 188-193
- [14] Bao Z, Lovinger A J, Dodabalapur A. *Adv. Mater.*, **1997**,**9**: 42-44
- [15] Horowitz G, Hajlaoui M E. *Adv. Mater.*, **2000**,**12**:1046-1050
- [16] Li Y, Chen S, Liu Q, et al. *J. Phys. Chem. C*, **2012**,**116**:4287-4292
- [17] Yang S Y, Shin K, Park C E. *Adv. Funct. Mater.*, **2005**,**15**: 1806-1814
- [18] Bräuer B, Kukreja R, Virkar A, et al. *Org. Electron.*, **2011**, **12**:1936-1942
- [19] Ye R, Baba M, Ohishi Y, et al. *Mol. Cryst. Liq. Cryst.*, **2006**,**444**:203-210
- [20] Li Y, Chen S, Liu Q, et al. *J. Phys. Chem. C*, **2014**,**118**: 14218-14226
- [21] Hu Y, Qi Q, Jiang C. *Appl. Phys. Lett.*, **2010**,**96**:133311
- [22] Schmidt R, Oh J H, Sun Y S, et al. *J. Am. Chem. Soc.*, **2009**,**131**:6215-6228
- [23] Acton O, Ting G G, Shamberger P J, et al. *ACS Appl. Mater. Interfaces*, **2010**,**2**:511-520
- [24] Yakuphanoglu F, Gunduz B. *Synth. Met.*, **2012**,**162**:1210-1239
- [25] Chen J, Tee C K, Shtein M, et al. *J. Appl. Phys.*, **2008**,**103**: 114513
- [26] Sung C, Kekuda D, Chu L F, et al. *Adv. Mater.*, **2009**,**21**: 4845-4849
- [27] Kobayashi S, Takenobu T, Mori S, et al. *Sci. Technol. Adv. Mater.*, **2003**,**4**:371-375
- [28] Anthopoulos T D, Singh B, Marjanovic N, et al. *Appl. Phys. Lett.*, **2006**,**89**:213504